"P. D. Burns and R. S. Berns, Modeling colorimetric error in electronic image acquisition, Proc. of Optics and Imaging in the Information Age, IS&T, 147-149, (1997).

Modeling Colorimetric Error in Electronic Image Acquisition

Peter D. Burns and Roy S. Berns*
Munsell Color Science Laboratory, Center for Imaging Science
Rochester Institute of Technology, Rochester, New York

Abstract

Electronic image acquisition systems not only detect optical signals but also convert them into a digital form for further image processing and exchange. We describe how a model of the detector can be combined with error-propagation analysis of the signal path, to predict the signal and noise characteristics of the digital image. The influence of a color-correction matrix on both the magnitude and interchannel correlation of detector noise is described for a charge-coupled device (CCD) imager and signal transformation to CIELAB.

Introduction

Digital color image acquisition systems usually comprise a detector, supporting electronics for signal readout and analog-to-digital conversion, and image processing to convert the image signal into a color-exchange or colorimetric representation. For example, to transform the camera red, green, and blue (*RGB*) signals to approximations of CIE tristimulus values (*XYZ*), a matrix operation is often used[1]

$$\mathbf{t} = \mathbf{M}\mathbf{s} \tag{1}$$

where

$$\mathbf{s}^T = [R\ G\ B],\ \mathbf{t}^T = [X\ Y\ Z]$$

M is a (3 × 3) matrix of weights, and the superscript, T, indicates matrix transpose. In most practical cases, the imager spectral sensitivities cannot be expressed as a linear combination of CIE color matching functions, therefore Eq. (1) allows only an approximation to the tristimulus values. As a consequence, the matrix **M** will be a function of the illuminant spectral power distribution and imager spectral sensitivities, and is chosen to minimize a particular weighting of colorimetric difference between the estimated and true tristimulus values.

All imaging detectors are subject to stochastic error due to, for example, photon arrival statistics (shot noise), thermally generated electrons, readout electronics and signal amplification. The detected signals, **s**, will therefore include variation from many sources, and can be modeled as a set of random variables. The transformed signal, **t**, contains a corresponding error that will be a function of the variation in **s**, and the matrix transformation, **M**. Error-propagation analysis[2] provides a way of predicting the statistics of the noise due to the image detection step in terms of the output transformed signal.

The second-order statistics of a set of detected signals subject to a stochastic error can be described by the covariance matrix,

$$\Sigma_s = \begin{bmatrix} \sigma_{RR} & \sigma_{RG} & \sigma_{RB} \\ \sigma_{RG} & \sigma_{GG} & \sigma_{GB} \\ \sigma_{RB} & \sigma_{GB} & \sigma_{BB} \end{bmatrix}$$

where the diagonal elements are the variance values of the *R*, *G* and *B* signals. In general the elements of Σ_s will be functions of the mean detected signal. The resulting covariance matrix for the transformed signals is[3]

$$\Sigma_t = \mathbf{M}\,\Sigma_s\,\mathbf{M}^T \tag{2}$$

Similarly, the propagation of the signal covariance through nonlinear transformations can be approximated by applying a derivative matrix. This is useful if the CIELAB coordinates are expressed as a vector, $c^T = [L^*a^*b^*]$, and the Jacobian Matrix† of the multivariate transformation is written as

$$\mathbf{J} = \begin{bmatrix} 0 & \partial L^*/\partial Y & 0 \\ \partial a^*/\partial X & \partial a^*/\partial Y & 0 \\ 0 & \partial b^*/\partial Y & \partial b^*/\partial Z \end{bmatrix}$$

then[4]

$$\Sigma_c \approx \mathbf{J}\,\Sigma_t\,\mathbf{J}^T \tag{3}$$

CCD Imager Noise Model

There are several sources of noise in charge-coupled device (CCD) imagers,[5,6] but for our purposes here, we will lump the net stochastic variations as being of two types: dark noise, whose variance is independent of signal level, and shot noise, whose variance is proportional to the (mean) signal. Note that these characteristics can be estimated from the published information for many detectors, which often includes values for RMS dark electrons, read noise, and shot-noise estimates based on full-signal charge. We will assume the fixed-pattern noise from variation in the sensor sensitivity is compensated for, and that the three image (R, G, B) records are fully populated having been sampled, or by previous interpolation.

As an example, consider the CCD imager detector/optics whose spectral sensitivities are shown in Figure 1. We assume shot-noise levels correspond to a maximum signal of 60,000 electrons/pixel. The RMS dark noise is taken as equivalent to 50 electrons, 0.08% of the maximum signal. These noise characteristics are shown in Figure 2, and expressed on the scale of [0-1]. The color-correction matrix was calculated to transform the detected signals to esti-

mates of tristimulus values. Given the spectral sensitivities of Figure 1, and a D65 illuminant, the matrix

$$\mathbf{M} = \begin{bmatrix} 0.321 & 0.666 & 0.425 \\ 0.106 & 1.140 & 0.125 \\ -0.039 & -0.076 & 4.399 \end{bmatrix} \quad (4)$$

is based on a set of 24 measurements of a Macbeth Color Checker chart, and can be applied as in Equation (1).

Table 1. Measured CIELAB coordinates for the 24 patches of the Macbeth ColorChecker, and the calculated CIELAB RMS errors following imager noise model.

Name	L^*	a^*	b^*	σ_{L^*}	σ_{a^*}	σ_{b^*}	$\overline{\Delta E^*_{ab}}$
Dark skin	37.9	14.7	14.9	0.28	0.63	1.69	1.53
Light skin	66.2	15.5	14.7	0.20	0.43	0.91	0.93
Blue sky	51.1	-6.48	-23.5	0.24	0.46	0.83	0.94
Foliage	44.4	-11.2	24.9	0.26	0.48	1.66	1.43
Blue flower	57.6	14.6	-24.8	0.21	0.47	0.77	0.90
Bluish green	73.0	-21.6	0.54	0.19	0.33	0.77	0.81
Orange	59.4	21.5	53.2	0.21	0.47	1.81	1.50
Purplish blue	41.0	9.58	-43.3	0.27	0.58	0.82	1.03
Moderate red	50.8	42.2	10.6	0.22	0.54	1.13	1.12
Purple	32.5	28.5	-19.1	0.30	0.74	1.16	1.30
Yellow grn.	74.3	-22.3	60.9	0.19	0.33	1.33	1.12
Orange yel.	71.4	8.13	65.5	0.19	0.40	1.56	1.30
Blue	29.5	12.5	-52.7	0.34	0.76	0.92	1.21
Green	57.6	-31.1	38.6	0.23	0.33	1.42	1.20
Red	43.1	66.4	29.4	0.22	0.61	1.95	1.66
Yellow	81.8	-2.33	80.3	0.18	0.35	1.51	1.25
Magenta	52.7	54.5	-12.9	0.20	0.53	0.87	0.97
Cyan	51.7	-11.8	-28.1	0.24	0.44	0.80	0.92
White	96.1	-3.65	1.82	0.16	0.33	0.65	0.73
Neutral 8	81.1	-3.61	-0.85	0.18	0.36	0.71	0.78
Neutral 6.5	66.2	-3.16	-0.64	0.20	0.40	0.82	0.87
Neutral 5	50.6	-2.66	-0.85	0.24	0.47	1.00	1.02
Neutral 3.5	33.7	-2.35	-0.67	0.31	0.63	1.4	1.41
Black	19.0	-0.80	-0.98	0.50	1.02	2.50	2.33

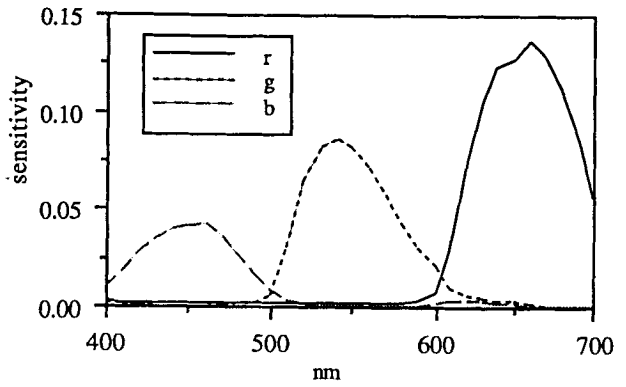

Figure 1. Spectral sensitivity functions of detector and optics, on a [0-1] scale.

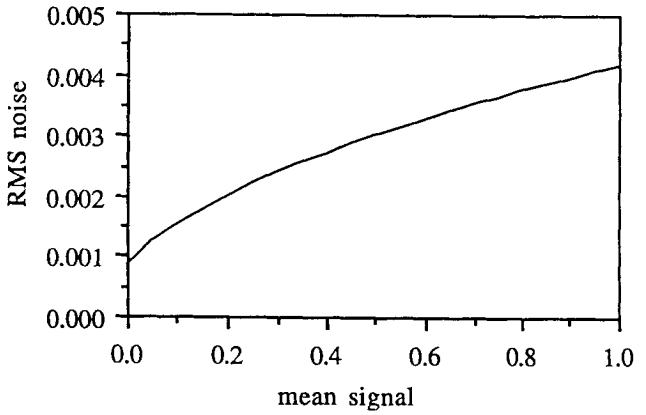

Figure 2. RMS noise characteristics for model imager, where signal and noise are expressed on a [0-1] scale.

For this example we assume that the set of *R,G,B* signals include independent noise fluctuations, whose RMS values vary with mean signal level as in Figure 2. The signal covariance, Σ_s is diagonal. The results of applying Equations (1) and (2) are given in Table 1, and predict areas in CIELAB with higher noise. The noise of the Black sample can be attributed to the high gain from the matrix **M** element, 4.399. This is because of the relatively low spectral sensitivity of the blue detection channel. The transformation from tristimulus values to CIELAB further emphasizes the dark signal fluctuations, due to the cube-root transformation and its derivative.

Although the matrix **M** is chosen to correct the *mean* camera signals, it has a direct influence, via Equation (2), on both the magnitude and correlation of the image *noise* in a transformed color space (e.g., tristimulus values or CIELAB). It is often assumed that if a set of camera spectral sensitivities are 'within a linear combination' of those desired, then they are acceptable, since camera signals can be corrected via Equation (1). When image noise is considered, however, we see that not all linear combinations are equivalent.

In our example, a higher blue-channel sensitivity would result in lower values of the coefficients in the third column of **M**, and reduced image noise levels in the transformed color-spaces. Alternatuvely, if modifying the spectral sensitivity of the detector-optics combination is not feasible, changing the detector or signal-readout scheme could reduce the image noise in the primary set of signals (R, G, B).

Conclusions

Modeling of the signal detection and noise characteristics of color-measurement and imaging devices can be combined with error-propagation analysis to predict signal uncertainty in color-exchange signals. Since physical devices include correlated noise sources, and signal-processing often combines signals, analysis of signal covariance is included. By applying these methods, design and calibration strategies can include not only the minimization of mean color errors, but also the signal variation.

The signal and noise requirements for image acquisition systems of this type are usually expressed in terms of the output, or transformed signal-space. The above analysis can be used to express the output image noise in terms of specific of design choices, such as illumination power, optical filters and detector. Errors due to variations in operating conditions, aging and manufacturing tolerances can also be analyzed if they are well described as stochastic processes. Noise levels modeled in this way can be compared with errors due to limited precision used in signal storage, and image processing.

Acknowledgement

We thank Richard Vogel of Eastman Kodak for his review of this paper and comments.

References

1. J. A. Quiroga, J. Zoido, J. Alonso, and E. Bernabeu, "Colorimetric Matching by Minimum-square-error fitting," *Appl. Opt.*, **33**: 6139-6141 (1994).
2. B. N. Taylor and C. E. Kuyatt, *Guidelines for evaluating and expressing the uncertainty of NIST measurement results, NIST Tech. Note 1297*, US Dept. of Commerce, Washington, 1993, p. 8.
3. R. A. Johnson and D. W. Wichern, *Applied Multivariate Statistical Analysis*, Prentice-Hall, Engelwood Cliffs, New Jersey, 1992, pp. 61-61.
4. P. D. Burns and R. S. Berns, "Error Propagation Analysis in Color Measurement and Imaging," submitted for publication.
5. T. W. McCurnin, L. C. Schooley and G. R. Sims, "Charge-Coupled Device Signal Processing Models and Comparisons," *J. Electronic Imaging*, **2**: 100-107 (1993).
6. P. D. Burns, "Image Signal Modulation and Noise Characteristics of Charge-coupled Device Imagers," *Proc. SPIE*, **1071**: 144-152 (1989).

* Address: Eastman Kodak Company, mail stop 01925, Rochester, NY 14650-1925 / pburns@kodak.com

† The Jacobian is the determinant of this matrix.